

Impact of annealing temperature on the ferroelectric properties of W/$Hf_{0.5}Zr_{0.5}O_2$/W capacitor

Dao Wang(王岛), Yan Zhang(张岩), Yongbin Guo(郭永斌), Zhenzhen Shang(尚真真), Fangjian Fu(符方健), and Xubing Lu(陆旭兵)

Citation: Chin. Phys. B, 2023, 32 (**9**): 097701. DOI: 10.1088/1674-1056/aca9c6
Journal homepage: http://cpb.iphy.ac.cn; http://iopscience.iop.org/cpb

What follows is a list of articles you may be interested in

Recent advances, perspectives, and challenges inferroelectric synapses

Bo-Bo Tian(田博博), Ni Zhong(钟妮), Chun-Gang Duan(段纯刚)
Chin. Phys. B, 2020, 29 (**9**): 097701. DOI: 10.1088/1674-1056/aba603

Structures and local ferroelectric polarization switching properties of orthorhombic $YFeO_3$ thin film prepared by a sol-gel method

Runlan Zhang(张润兰), Shuaishuai Li(李帅帅), Changle Chen(陈长乐), Li-An Han(韩立安), Shanxin Xiong(熊善新)
Chin. Phys. B, 2019, 28 (**3**): 037701. DOI: 10.1088/1674-1056/28/3/037701

Optimization of TiO_2/Cu/TiO_2 multilayers as a transparent composite electrode deposited by electron-beam evaporation at room temperature

Sun Hong-Tao (孙洪涛), Wang Xiao-Ping (王小平), Kou Zhi-Qi (寇志起), Wang Li-Jun (王丽军), Wang Jin-Ye (王金烨), Sun Yi-Qing (孙义清)
Chin. Phys. B, 2015, 24 (**4**): 047701. DOI: 10.1088/1674-1056/24/4/047701

Effects of O_2/Ar ratio and annealing temperature on electrical properties of Ta_2O_5 film prepared by magnetron sputtering

Huang Shi-Hua (黄仕华), Cheng Pei-Hong (程佩红), Chen Yong-Yue (陈勇跃)
Chin. Phys. B, 2013, 22 (**2**): 027701. DOI: 10.1088/1674-1056/22/2/027701

Optimized growth and dielectric properties of barium titanate thin films on polycrystalline Ni foils

Liang Wei-Zheng(梁伟正), Ji Yan-Da(吉彦达), Nan Tian-Xiang(南天翔), Huang Jiang(黄江), Zeng Hui-Zhong(曾慧中), Du Hui(杜辉), Chen Chong-Lin(陈充林), and Lin Yuan(林媛)
Chin. Phys. B, 2012, 21 (**6**): 067701. DOI: 10.1088/1674-1056/21/6/067701

Impact of annealing temperature on the ferroelectric properties of W/$Hf_{0.5}Zr_{0.5}O_2$/W capacitor

Dao Wang(王岛)[1,3], Yan Zhang(张岩)[2,3,†], Yongbin Guo(郭永斌)[4], Zhenzhen Shang(尚真真)[1], Fangjian Fu(符方健)[1], and Xubing Lu(陆旭兵)[3,‡]

[1] *College of Science, Qiongtai Normal University, Key Laboratory of Child Cognition and Behavior Development of Hainan Province, Haikou* 571127, *China*
[2] *College of Electronic and Electrical Engineering, Henan Normal University, Xinxiang* 453007, *China*
[3] *Institute for Advanced Materials and Guangdong Provincial Key Laboratory of Quantum Engineering and Quantum Materials, South China Academy of Advanced Optoelectronics, South China Normal University, Guangzhou* 510006, *China*
[4] *Key Laboratory of UWB and THz of Shandong Academy of Sciences, Institute of Automation, Qilu University of Technology (Shandong Academy of Sciences), Jinan* 250014, *China*

(Received 30 August 2022; revised manuscript received 23 November 2022; accepted manuscript online 8 December 2022)

Crystallization annealing is a crucial process for the formation of the ferroelectric phase in HfO_2-based ferroelectric thin films. Here, we systematically investigate the impact of the annealing process, with temperature varied from 350 °C to 550 °C, on the electricity, ferroelectricity and reliability of a $Hf_{0.5}Zr_{0.5}O_2$ (HZO; 7.5 nm) film capacitor. It was found that HZO film annealed at a low temperature of 400 °C can effectively suppress the formation of the monoclinic phase and reduce the leakage current. HZO film annealed at 400 °C also exhibits better ferroelectric properties than those annealed at 350 °C and 550 °C. Specifically, the 400 °C-annealed HZO film shows an outstanding $2P_r$ value of 54.6 μC·cm^{-2} at ±3.0 MV·cm^{-1}, which is relatively high compared with previously reported values for HZO film under the same electric field and annealing temperature. When the applied electric field increases to ±5.0 MV·cm^{-1}, the $2P_r$ value can reach a maximum of 69.6 μC·cm^{-2}. In addition, the HZO films annealed at 400 °C and 550 °C can endure up to bout 2.3×10^8 cycles under a cycling field of 2.0 MV·cm^{-1} before the occurrence of breakdown. In the 400 °C-annealed HZO film, 72.1% of the initial polarization is maintained while only 44.9% is maintained in the 550 °C-annealed HZO film. Our work demonstrates that HZO film with a low crystallization temperature (400 °C) has quite a high ferroelectric polarization, which is of significant importance in applications in ferroelectric memory and negative capacitance transistors.

Keywords: $Hf_{0.5}Zr_{0.5}O_2$ thin film, annealing temperature, ferroelectric polarization, endurance

PACS: 77.84.–s, 85.50.Gk, 77.55.D–, 77.55.fp **DOI:** 10.1088/1674-1056/aca9c6

1. Introduction

Recently, HfO_2-based ferroelectric thin films, especially $Hf_{0.5}Zr_{0.5}O_2$ (HZO) film, have attracted much attention for application in non-volatile ferroelectric memory, ultralow-power logic devices and neuromorphic computing.[1–5] Such films have the advantages of a large bandgap (5.2–5.8 eV), excellent compatibility with the complementary metal–oxide–semiconductor (CMOS) process and high scalability compared with traditional perovskite-structure ferroelectric materials.[1–3] Generally, the spontaneous polarization in HfO_2-based ferroelectric materials originates from a non-centrosymmetric orthorhombic phase (o-phase; $Pca2_1$).[1–5] The formation and stability of the ferroelectric o-phase in films are affected by various factors, such as large tensile strain and a proper annealing process.[1–3] The annealing temperature of HZO ferroelectric thin film is reported to vary between 300 °C and 800 °C.[6–20] To improve the ferroelectric properties, most researchers have adopted high-temperature (≥ 500 °C) treatment methods for generating stresses in the film.[9–14]

This high thermal budget process not only degrades the qualities of HZO film but also restricts its integration in the back end of line (BEOL) circuits in CMOS technology.[15–21] Therefore, it is necessary for HZO-based devices to achieve reasonable ferroelectric properties via a low-temperature annealing process so that they can be used in the above technologies.[19] However, when HZO film crystallizes in a low-temperature (e.g., 300 °C–450 °C) annealing process or without any heat treatment it exhibits relatively low remnant polarization (initial $2P_r$ = 5–40 μC·cm^{-2}),[15–21] which is unacceptable for various practical applications.

The ferroelectricity of HZO thin film can significantly decrease as the annealing temperature goes down to 400 °C or lower,[16,17,19] which is ascribed to the non-ferroelectric phase or amorphous phase becoming dominant and the formation of the o-phase being strongly suppressed.[16,17] It has been reported that the generation and stability of the o-phase are closely related to the mechanical clamping strain exerted by the capping layers (or top electrodes), whereas the magnitude of the strain depends on the difference in the thermal expansion coefficient (TEC) between the top and bottom electrodes or between the electrodes and ferroelectric films.[22–25] Therefore, to effectively stabilize the ferroelectric o-phase of HZO

[†]Corresponding author. E-mail: 1053527200@qq.com
[‡]Corresponding author. E-mail: luxubing@m.scnu.edu.cn

© 2023 Chinese Physical Society and IOP Publishing Ltd

film and maintain a low thermal budget, it is necessary to select metal capping electrodes with a relatively low TEC to enhance the in-plane tensile strain on the HZO film.[15,16,18,22] It is noteworthy that tungsten (W) electrode has excellent chemical stability and a lower TEC (4.5×10^{-6} K^{-1}),[22,23] which can produce a high in-plane tensile strain and suppress interface defects. This could not only stabilize the ferroelectric o-phase but also reduce the leakage current.[26,27] Therefore, W electrode is expected to induce large in-plane tensile strain under a low thermal budget, resulting in the formation of a high o-phase content and improving the reliability of the HZO film.

In this paper, we carried out a systematic study on the electrical, ferroelectric and fatigue properties of HZO film deposited on a W electrode with different annealing temperatures (350 °C–550 °C). It is observed that the 400 °C-annealed HZO film exhibits outstanding ferroelectricity with a $2P_r$ value of 54.6 μC·cm^{-2} at ±3.0 MV·cm^{-1}, which is larger than previously reported values for HZO film. These results indicate that annealing at temperatures as low as 400 °C could result in the crystallization of HZO film showing superior ferroelectric properties, which is of great significance for applications in memory devices and negative capacitance transistors.

2. Experimental methods

A schematic diagram of a metal–ferroelectric–metal capacitor is shown in the inset of Fig. 1(a). First, a ∼ 50-nm thick W bottom electrode (BE) was deposited on top of the Si/SiO_2 (100) substrate by sputtering. Next, a ∼ 7.5-nm thick HZO thin film was deposited on the W BE using thermal atomic layer deposition (ALD) at 280 °C with a Hf:Zr = 1:1 cycle ratio. Hf[$N(CH_3)_2$]$_4$, Zr[$N(CH_3)_2$]$_4$ and O_3 were used as the Hf precursor, Zr precursor and oxygen source, respectively. For the electrical characterization, a ∼ 50-nm thick W top electrode (TE) was deposited by sputtering through a shadow mask to create circular contact pads of diameter 100 μm. Finally, the W/HZO/W capacitor was annealed by rapid thermal annealing (RTA) at 350 °C, 400 °C and 550 °C in a N_2 atmosphere for 30 s. X-ray reflectivity (XRR) and grazing incidence x-ray diffraction (GIXRD) measurements were carried out with a PANalytical X'Pert Pro diffractometer for analysis of thickness and structural phase of the HZO film. Electrical measurements, such as the polarization–voltage (P–V), capacitance–voltage (C–V) and current–voltage (I–V) characteristics, were measured using a ferroelectric tester (Radiant Technology, Precision LC II), an impedance analyzer (Keysight, E4990A) and a semiconductor parameter analyzer (Agilent, B1500A), respectively.

3. Results and discussion

The XRR spectrum of an as-grown HZO film is presented in Fig. 1(a), and its thickness is determined to be about 7.5 nm. It is well known that doped HfO_2 film is composed of a monoclinic phase (m-phase), a tetragonal-phase (t-phase) and an o-phase.[1–5] Among these phases, the o-phase is considered to be the prime reason for the ferroelectricity in HZO film.[3,5] Generally, the m-phase for HZO film is located at around 2θ values of 28.5° and 31.5° whereas the o-phase and t-phase are located at around 30.5°.[3] The GIXRD technique was also adopted for understanding the crystal structures of HZO film at various annealing temperatures, as shown in Fig. 1(b). As-deposited HZO film was mostly amorphous or contained only a small portion of very fine crystalline nuclei with a size of about 2 nm.[9,28] No peak was observed in the 350 °C-annealed HZO film, indicating its amorphous state or weak crystallinity.[29] When the RTA temperature was 400 °C, the two peaks at $2\theta = 28.5°$ and 31.5°, corresponding respectively to m(–111) and m(111) planes, were not shown in the patterns, while the main peak of the o/t(111) phase at $2\theta = 30.5°$ was observed, indicating that the major crystalline phases of the 400 °C-annealed HZO films was the o/t mixed phase.[3,5,6] This is because the tiny nuclei (∼ 2 nm radius) formed *in situ* during the ALD process will most probably have the t-phase structure, which will serve as the crystallization seed for the entire film into the t-phase during RTA.[9,28] The supposed transition to the m-phase at the achieved grain size would be suppressed by the high activation barrier, and retained t-phase would be changed to the desired o-phase during cooling.[9,28] With temperature further increasing to 550 °C or above, the intensity of the diffraction peak at 28.5° is slightly enhanced, which corresponds to the increase in the relative fraction of the m(–111) phase, resulting in a decrease in the P_r value.[3,9,22] This is because the transition to the m-phase was kinetically enhanced at high temperature while the stability of the m-phase decreases thermodynamically at high temperature.[9] Thus, there is a transition from the o-phase to the m-phase in the HZO films with increase in the RTA temperature, and the proportion of m-phase increases with increase in the annealing temperature.[9,28]

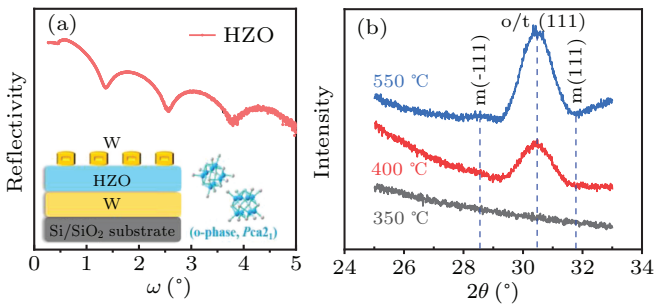


Fig. 1. (a) XRR spectrum of as-deposited HZO film. (b) GIXRD patterns of HZO film annealed at different temperatures (350 °C, 400 °C and 550 °C). The inset shows a schematic diagram of a W/HZO/W capacitor.

Figures 2(a)–2(c) present the polarization–electric field (P–E) characteristics of a W/HZO/W capacitor annealed at 350 °C, 400 °C and 550 °C, respectively. In Fig. 2(a), the

350 °C-annealed HZO film exhibits a linear dielectric behavior without ferroelectric properties, which is due to the existence of the amorphous state.[18,29] The 400 °C- and 550 °C-annealed HZO films display hysteresis loops in the *P*–*E* curves and a characteristic transformation from a linear response behavior to a well saturated ferroelectric hysteresis when the sweeping field is gradually increased from ±1.0 MV·cm^{-1} to ±5.0 MV·cm^{-1} (see Figs. 2(b) and 2(c)). Clearly, the breakdown field of *P*–*E* loops for 400 °C-annealed HZO film is higher (5.0 MV·cm^{-1}) than that of 550 °C-annealed HZO film (4.0 MV·cm^{-1}). The saturation polarization (P_s), $2P_r$ and coercive field ($2E_c$) values for HZO film annealed at the three temperatures were extracted from *P*–*E* hysteresis loops, respectively, as shown in Figs. 2(d)–2(f). In Figs. 2(d) and 2(e), it can be clearly observed that the P_s and $2P_r$ values of 400 °C-annealed HZO film are slightly higher over the entire field range than those of 550 °C-annealed HZO film. This is because the 400 °C-annealed HZO film forms more o/t-phases than those annealed at 550 °C and 350 °C, as already confirmed by GIXRD (see Fig. 1(b)). In addition, the 400 °C-annealed HZO film shows an extremely high $2P_r$ value of ∼ 60.5 μC·cm^{-2} at ±4.0 MV·cm^{-1}, and its maximum value can reach 69.6 μC·cm^{-2} at ±5 MV·cm^{-1}. From Fig. 2(f), the $2E_c$ of 400 °C-annealed HZO film is larger than those of the 350 °C- and 550 °C-annealed HZO films. These excellent ferroelectric properties are beneficial in various practical applications.

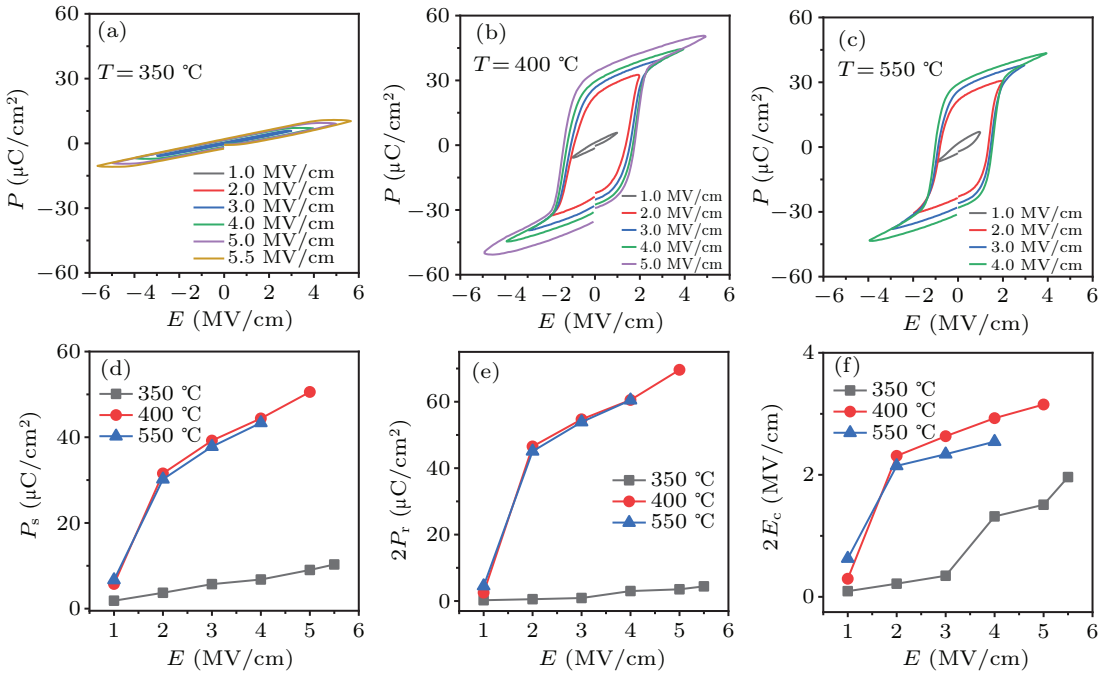


Fig. 2. Polarization–electric field (*P*–*E*) hysteresis loops of HZO film annealed at 350 °C (a), 400 °C (b) and 550 °C (c). Comparison of (d) P_s, $2P_r$ (e) and (f) $2E_c$ of these HZO samples.

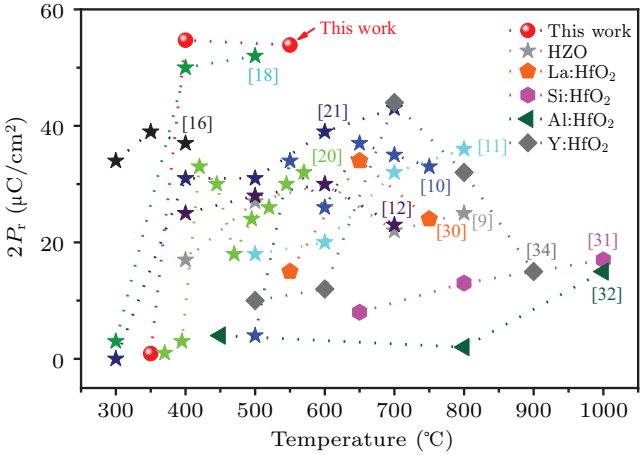


Fig. 3. Comparison of ferroelectric polarization between this work and previous HfO_2-based capacitors (note: data were obtained from the references and plotted by the authors).

The $2P_r$ values at ±3.0 MV·cm^{-1} for the doped-HfO_2 ferroelectric thin films as a function of annealing temperature are summarized in Fig. 3. The HZO films commonly showed a high $2P_r$ value in the low annealing temperature range of 300–800 °C,[6–20] while the data for La-,[30] Si-,[31] Al-[32,33] and Y-doped[34] HfO_2 films were located above 600 °C. This is deemed to be related to the formation temperature of ferroelectric o-phase. The annealing temperature of doped HfO_2 film is high, which can be attributed to the crystallization temperature of La_2O_3, SiO_2, Al_2O_3 and Y_2O_3 being higher than that of ZrO_2.[35–40] In addition, it was observed that the $2P_r$ value of HZO film exhibited large fluctuations with increase in annealing temperature, suggesting that a difference in the volume fraction of the ferroelectric o-phase occurs. It is clear that the crystallization temperatures of our HZO film are reflected in a lower annealing temperature of 400 °C while maintaining a superior $2P_r$ value of 54.6 μC·cm^{-2}. This $2P_r$ value

is the largest of any previously reported for HZO ferroelectric film.[9–21] This implies that HZO-based ferroelectric circuits with a low thermal budget can now be integrated into the BEOL for multi-functional memory devices or used for next-generation flexible and wearable products.[16–19]

To investigate the effects of various annealing temperatures on the electrical properties of HZO films, current and capacitance measurements were performed. Figure 4(a) shows the leakage current density–electric field (J–E) properties obtained from W/HZO/W capacitors with several annealing temperatures. The 350 °C-annealed HZO film displays a remarkably low J value compared with those for HZO films annealed at 400 °C and 550 °C, which is attributed to its amorphous state (confirmed by the GIXRD results) or no grain boundaries. Additionally, a slightly higher J value was observed in the 550 °C-annealed HZO film than in the 400 °C-annealed HZO film. The breakdown field of the HZO film capacitor gradually decreased from 5.5 MV·cm^{-1} to 4.0 MV·cm^{-1} with a further increase in annealing temperature. There are a number of reasons for this. First, the leakage current generally passed through the grain boundaries of crystalline HZO films.[16,38,41] Therefore, the increase in J value is due to the grain boundaries being more clearly formed with increasing annealing temperature. Second, the parasitic oxidized interface between the electrode and dielectric layer is mainly attributed to oxygen scavenging by the electrode from the ferroelectric layer during the annealing treatment.[7] The oxygen scavenging effect is enhanced with increasing annealing temperature, which leads to an increase in the thickness of the interfacial layer.[42,43] However, the interfacial layer can contain a high defect density (e.g., V_O) and the charges may be easily injected, which can cause charge trapping at defect sites or even generate additional defects.[7] Accordingly, these charges can affect the leakage current.[44] Therefore, it could be conjectured that the thickness of the WO_x interfacial layer formed and the accumulation of oxygen vacancies at an annealing temperature of 550 °C are higher than those for annealing at 350 °C and 400 °C, resulting in a high leakage current. Figure 4(b) shows the dielectric constant versus electric field (ε_r–E) curves of HZO film with different annealing temperatures, extracted from the capacitance measurements. It can be observed that the 350 °C-annealed HZO film does not exhibit the typical ε_r–E butterfly shape, corresponding to the suppression of ferroelectric properties.[29] On the other hand, the ε_r–E curves of the 400 °C- and 550 °C-annealed HZO film present the butterfly-like shape which is a typical ferroelectric characteristic.[16] The ε_r values of 350 °C-, 400 °C- and 550 °C-annealed HZO films at −3.0 MV·cm^{-1} are 20, 31 and 30, respectively. Given that the relative permittivity of the o-phase is typically higher than those of m- and amorphous-phases,[45] it is expected that the o-phase would be more dominant relative to the other phases in the HZO film annealed at 400 °C.

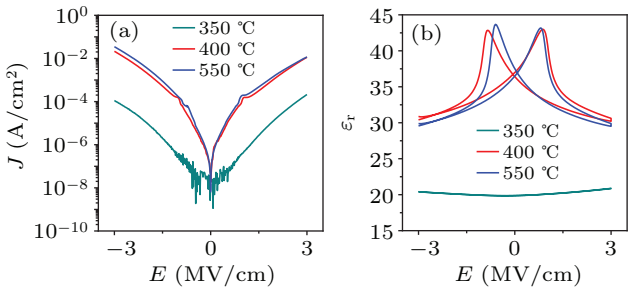


Fig. 4. (a) The J–E curves and (b) ε_r–E curves of HZO film annealed at different temperatures.

In order to give a full picture of the fatigue properties, cycling endurance tests with 400 °C- and 550 °C-annealed HZO films were performed with different field amplitudes, and the results are presented in Figs. 5(a) and 5(b). The amplitude of cycling field/PUND read pulses was set at 1.33/2.0 MV·cm^{-1}, 2.0/2.0 MV·cm^{-1} and 2.67/2.67 MV·cm^{-1}, respectively. When a low cycle field of 1.33 MV·cm^{-1} was applied, the 400 °C- and 550 °C-annealed HZO films demonstrated endurance performance up to 5.2×10^9 cycles and 3.7×10^9 cycles without breakdown. This is attributed to the fact that fatigue is a subcycling process, and there is partial of the ferroelectric dipoles were incompletely polarization switching.[46] It is well known that the fatigue characteristics also depend on the cycling electric field.[47] At a cycling field of 2.0 MV·cm^{-1} the ferroelectric HZO film shows the characteristic fatigue behavior of ferroelectric materials. Both the 400 °C- and 550 °C-annealed HZO films can endure up to $\sim 2.3\times10^8$ cycles before breakdown. For 400 °C-annealed HZO film 72.1% of the initial polarization is maintained, while only 44.9% is maintained for the 550 °C-annealed HZO film. For a high field strength of 2.67 MV·cm^{-1}, both the 400 °C- and 550 °C-annealed HZO films suffered from early breakdown at $\sim 10^6$ cycles, but their fatigue rates were different. Therefore, the fatigue properties of the 400 °C-annealed HZO film are better than those of the 550 °C-annealed HZO film. The reasons for the difference in fatigue properties between 400 °C- and 550 °C-annealed HZO films are as follows. First, the breakdown and fatigue in ferroelectric films are closely related to the leakage current, because the leakage current induces cumulative Joule heating and charge trapping effects during the repeated endurance cycles.[48,49] Therefore, it can be anticipated that the better performance of the 400 °C-annealed HZO film against breakdown and fatigue might be due to the decreased leakage current, as indeed confirmed by Fig. 4(a). Secondly, the hard breakdown is a primary failure mechanism of doped HfO_2, and is strongly influenced by the diffusion and accumulation of oxygen vacancies.[50,51] The low concentration of oxygen vacancies should be beneficial for

achieving a large electric field cycle number and slow fatigue rates until breakdown.[12] Therefore, crystallization at a lower temperature of 400 °C can be more effective in achieving a lower concentration of oxygen vacancies in the pristine state. Thirdly, high annealing temperatures can result in the formation of the partial m-phase, which can also affect the ferroelectric properties and endurance.[52] This is because the m-phase can work as a dead layer in ferroelectrics leading to the loss of the switching electric field across the m-phase, and an even higher field is necessary to induce sufficient electrical switching,[52] resulting in a degradation of both the ferroelectric properties and the endurance of the HZO capacitors. To the best of our knowledge, most studies have reported that the endurance of doped HfO_2 ferroelectric films reaches 10^8–10^{12} cycles at a cycling field of 2.0–3.5 MV·cm^{-1}.[1,2,8,53–56] Our fatigue results show some disadvantages compared with existing reports, and therefore further research is needed. Figure 5(c) shows the results of retention measurement for HZO film with write/read pulses of 2.5 MV·cm^{-1} and a 1 ms pulse width. Both samples showed similar trends of strong retention characteristics between 10^0 s and 10^4 s. After 1.3×10^4 s, the amount of polarization remaining in the 400 °C-annealed HZO film capacitor is 86%, which is slightly better than for the 550 °C-annealed HZO films capacitor (84%). These results infer that the WO_x interface layer between the HZO film and W electrode is easier to form at an elevated temperature up to 550 °C, resulting in the existence of a depolarization field in the HZO film[57,58] which degrades the long-term retention.

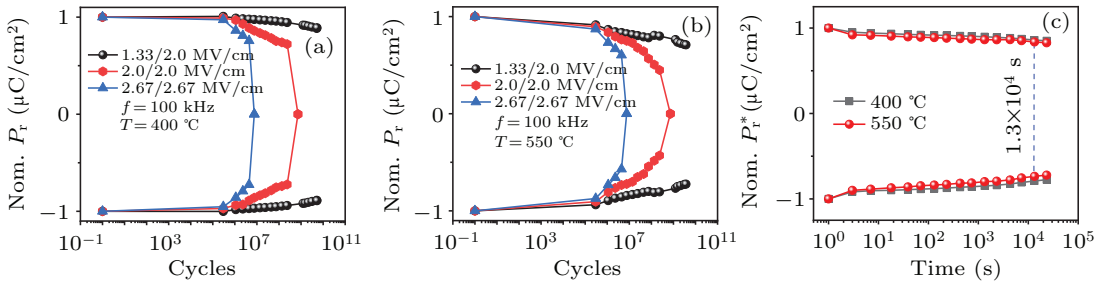


Fig. 5. Reliability measurement results of the HZO films annealed at various temperatures: fatigue characteristics of (a) 400 °C- and (b) 550 °C-annealed HZO films were recorded with different write/read pulses: 1.33/2.0 MV·cm^{-1}, 2.0/2.0 MV·cm^{-1} and 2.67/2.67 MV·cm^{-1}, respectively. (c) Retention properties.

4. Conclusions

In this work, the crystalline phase, ferroelectricity and reliability of HZO thin films annealed at several temperatures are systematically investigated. It is found that the 400 °C-annealed HZO film shows superior ferroelectric characteristics featuring a large switching polarization compared with the 350 °C- and 550 °C-annealed HZO films. An excellent $2P_r$ value of 54.6 μC·cm^{-2} at ±3.0 MV·cm^{-1} is observed for 400 °C-annealed HZO film, which is larger than previously reported values for HZO film under the same electric field and heat treatment temperature. According to the GIXRD analysis and ε_r value, this may be due to the formation of o/t-phases without the paraelectric m-phase of 400 °C-annealed HZO film. In addition, when a cycling field of 2.0 MV·cm^{-1} was applied, the 400 °C-annealed HZO film can endure up to $\sim 2.3\times10^8$ cycles and maintain 72.1% of its initial polarization before the occurrence of breakdown. Our fatigue results show some disadvantages compared with the fatigue properties of the currently reported doped HfO_2 films, and need to be further improved. This work demonstrated that annealing at temperatures as low as 400 °C could result in crystallization of HZO films showing sufficient ferroelectric polarization switching, which will contribute to their future applications in ferroelectric memory and negative capacitance transistors.

Acknowledgements

Project supported by Hainan Provincial Natural Science Foundation of China (Grant No. 523QN257), College-level Scientific Research Foundation of Qiongtai Normal University (Grant No. qtqn202215), the Innovation and Entrepreneurship Training Program for College Students (Grant No. 202213811016), Science and Technology Program of Henan (Grant No. 232102210182), Scientific Research Foundation of Henan Normal University (Grant No. 20230196), Natural Science Foundation of Shandong Province (Grant No. ZR2023QA047), Foundation of PeiXin (Grant No. 2023PX027), Science and technology smes innovation ability improvement project (Grant No. 2023TSGC0154), and the National Natural Science Foundation of China (Grant No. 62174059).

References

[1] Chen H Y, Zhou X F, Tang L, Chen Y H, Luo H, Yuan X, Bowen C R and Zhang D 2022 *Appl. Phys. Rev.* **9** 011307
[2] Ali F, Ali T, Lehninger D, Sünbül A, Viegas A, Sachdeva R, Abbas A, Czernohorsky M and Seidel K 2022 *Adv. Funct. Mater.* **32** 2201737
[3] Zhao D, Chen Z B and Liao X Z 2022 *Microstructures* **2** 2022007
[4] Migita S, Ota H, Shibuya K, Yamada H, Sawa A, Matsukawa T and Toriumi A 2019 *Jpn. J. Appl. Phys.* **58** SBBA07
[5] Park M H, Lee Y H, Kim H J, Kim Y J, Moon T, Kim K D, Müller J, Kersch A, Schroeder U, Mikolajick T and Hwang C S 2015 *Adv. Mater.* **27** 1811
[6] Kim S J, Mohan J, Summerfelt S R and Kim J 2018 *JOM* **71** 246

[7] Park M H, Lee D H, Yang K, Park J Y, Yu G T, Park H W, Materano M, Mittmann T, Lomenzo P D, Mikolajick T, Schroeder U and Hwang C S 2020 *J. Mater. Chem. C* **8** 10526

[8] Kim H J, An Y, Jung Y C, Mohan J, Yoo J G, Kim Y I, Hernandez-Arriaga H, Kim H S, Kim J and Kim S J 2021 *Phys. Status. Solidi. RRL* **15** 2100028

[9] Park M H, Lee Y H, Kim H J, Kim Y J, Moon T, Kim K D, Hyun S D, Mikolajick T, Schroeder U and Hwang C S 2018 *Nanoscale* **10** 716

[10] Lin Y C, McGuire F and Franklin A D 2018 *J. Vac. Sci. Technol. B* **36** 011204

[11] Mittmann T, Fengler F P G, Richter C, Park M H, Mikolajick T and Schroeder U 2017 *Microelectron. Eng.* **178** 48

[12] Park M H, Kim H J, Kim Y J, Lee W, Moon T and Hwang C S 2013 *Appl. Phys. Lett.* **102** 242905

[13] Yoon J S, Tewari A, Shin C and Jeon S 2019 *IEEE Electron. Device Lett.* **40** 1076

[14] Lee Y, Hsain H A, Fields S S, Jaszewski S T, Horgan M D, Edgington P G, Ihlefeld J F, Parsons G N and Jones J L 2021 *Appl. Phys. Lett.* **118** 012903

[15] Kim S J, Mohan J, Lee J, Lee J S, Lucero A T, Young C D, Colombo L, Summerfelt S R, San T and Kim J 2018 *Appl. Phys. Lett.* **112** 172902

[16] Onaya T, Nabatame T, Sawamoto N, Ohi A, Ikeda N, Nagata T and Ogura A 2019 *Microelectron. Eng.* **215** 111013

[17] Li Y X, Liang R R, Wang J B, Zhang Y, Tian H, Liu H F, Li S L, Mao W Q, Pang Y, Li Y T, Yang Y and Ren T L 2017 *IEEE J. Electron. Devices. Soc.* **5** 378

[18] Kim S J, Narayan D, Lee J, Mohan J, Lee J S, Lee J, Kim H S, Byun Y C, Lucero A T, Young C D, Summerfelt S R, San T, Colombo L and Kim J 2017 *Appl. Phys. Lett.* **111** 242901

[19] Gaddam V, Das D, Jung T and Jeon S 2021 *IEEE Electron. Device Lett.* **42** 812

[20] Persson A E O, Athle R, Littow P, Persson K M, Svensson J, Borg M and Wernersson L E 2020 *Appl. Phys. Lett.* **116** 062902

[21] Toprasertpong K, Tahara K, Fukui T, Lin Z Y, Watanabe K, Takenaka M and Takagi S 2020 *IEEE Electron. Device Lett.* **41** 1588

[22] Goh Y, Hwang J, Lee Y, Kim M and Jeon S 2020 *Appl. Phys. Lett.* **117** 242901

[23] Wang D, Zhang Y, Wang J L, Luo C L, Li M, Shuai W T, Tao R Q, Fan Z, Chen D Y, Zeng M, Dai J Y, Lu X B and Liu J M 2022 *J. Mater. Sci. Technol.* **104** 1

[24] Kashir A, Kim H, Oh S and Hwang H 2021 *ACS. Appl. Electron. Mater.* **3** 629

[25] Shiraishi T, Katayama K, Yokouchi T, Shimizuc T, Oikawa T, Sakata O, Uchida H, Imaie Y, Kiguchi T, Konno T J and Funakubo H 2017 *Mater. Sci. Semicond. Proc.* **70** 239

[26] Kashir A, Kim H, Oh S and Hwang H 2021 *ACS Appl. Electron. Mater.* **3** 629

[27] Kim H, Kashir A, Oh S and Hwang H 2021 *Nanotechnology* **32** 055703

[28] Park M H, Lee Y H, Mikolajick T, Schroeder U and Hwang C S 2019 *Adv. Electron. Mater.* **5** 1800522

[29] Oh S, Kim H, Kashir A and Hwang H 2020 *Appl. Phys. Lett.* **117** 252906

[30] Chernikova A G, Kuzmichev D S, Negrov D V, Kozodaev M G, Polyakov S N and Markeev A M 2016 *Appl. Phys. Lett.* **108** 242905

[31] Mueller S, Muller J, Schroeder U and Mikolajick T 2013 *IEEE Trans. Device. Mater. Reliab.* **13** 93

[32] Mueller S, Mueller J, Singh A, Riedel S, Sundqvist J, Schroeder U and Mikolajick T 2012 *Adv. Funct. Mater.* **22** 2412

[33] Yau H M, Chen X X, Wong C M, Chen D Y and Dai J Y 2021 *Mater. Charact.* **176** 111114

[34] Wang J J, Zhou D Y, Dong W, Yao Y F, Sun N, Ali F Z, Hou X D and Liu F 2021 *Adv. Electron. Mater.* **7** 2000585

[35] Yang C, Fan H Q, Qiu S J, Xi Y X and Fu Y F 2009 *J. Non-Cryst. Solids.* **355** 33

[36] Onaya T, Nabatame T, Sawada T, Kurishima K, Sawamoto N, Ohi A, Chikyow T and Ogura A 2016 *ECS Trans.* **75** 667

[37] Onaya T, Nabatame T, Sawada T, Kurishima K and Sawamoto N 2018 *Thin. Solid. Films.* **655** 48

[38] Martin D, Grube M, Weinreich W, Müller J, Weber W M, Schröder U, Riechert H and Mikolajick T 2013 *J. Appl. Phys.* **113** 194103

[39] Niinistö J, Kukli K, Heikkilä M, Ritala M and Leskelä M 2019 *Adv. Eng. Mater.* **11** 223

[40] Zheng Q S, Liu Y C, Li M, Liu Z G, Hu Y H, Zhang X W, Deng W and Wang M T 2020 *J. Eur. Ceram. Soc.* **40** 463

[41] Chen K T, Chen H Y, Liao C Y, Siang G Y, Lo C, Liao M H, Li K S, Chang S T and Lee M H 2019 *IEEE Electron. Device Lett.* **40** 399

[42] Hamouda W, Lubin C, Ueda S, Yamashita Y, Renault O, Mehmood F, Mikolajick T, Schroeder U, Negrea R and Barrett N 2020 *Appl. Phys. Lett.* **116** 252903

[43] Hamouda W, Pancotti A, Lubin C, Tortech L, Richter C, Mikolajick T, Schroeder U and Barrett N 2020 *J. Appl. Phys.* **127** 064105

[44] Materano M, Lomenzo P D, Kersch A, Park M H, Mikolajick T and Schroeder U 2021 *Inorg. Chem. Front.* **8** 2650

[45] Grimley E D, Schenk T, Sang X H, Pešić M, Schroeder U, Mikolajick T and LeBeau J M 2016 *Adv. Electron. Mater.* **2** 1600173

[46] Li S D, Zhou D Y, Shi Z X, Hoffmann M, Mikolajick T and Schroeder U 2020 *Adv. Electron. Mater.* **6** 2000264

[47] Ryu H, Xu Kai, Kim J H, Kang S, Guo J and Zhu W J 2019 *IEEE Trans. Electron Devices* **66** 2359

[48] Pesic M, Fengler F P G, Larcher L, Padovani A, Schenk T, Grimley E D, Sang X, LeBeau J M, Slesazeck S, Schroeder U and Mikolajick T 2016 *Adv. Funct. Mater.* **26** 4601

[49] Grimley D, Schenk T, Sang X, Pesic M, Schroeder U, Mikolajick T and LeBeau J M 2016 *Adv. Electron. Mater.* **2** 1600173

[50] Kozodaev M G, Chernikova A G, Korostylev E V, Park M H, Khakimov R R, Hwang C S and Markeev A M 2019 *J. Appl. Phys.* **125** 034101

[51] Mittmann T, Materano M, Lomenzo P D, Park M H, Stolichnov I, Cavalieri M, Zhou Z C, Chung C C, Jones J L, Szyjka T, Müller M, Kersch A, Mikolajick T and Schroeder U 2019 *Adv. Mater. Interfaces* **6** 1900042

[52] Park M H, Kim H J, Kim Y J, Jeon W, Moon T and Hwang C S 2014 *Phys. Status Solidi RRL* **8** 532

[53] Chernikova A G, Kozodaev M G, Negrov D V, Korostylev E V, Park M H, Schroeder U, Hwang C S and Markeev A M 2018 *ACS Appl. Mater. Interfaces* **10** 2701

[54] Cao R R, Song B, Shang D S, Yang Y, Luo Q, Wu S Y, Li Y, Wang Y, Lv H B, Liu Q and Liu M 2019 *IEEE Electron Device Lett.* **40** 1744

[55] Mulaosmanovic H, Breyer T E, Dünkel S, Beyer S, Mikolajick T and Slesazeck S 2021 *Nanotechnology* **32** 502002

[56] Peng Y, Xiao W W, Liu Y, Jin C J, Deng X R, Zhang Y Y, Liu F N, Zheng Y Z, Cheng Y, Chen B, Yu X, Hao Y and Han G Q 2022 *IEEE Electron Device Lett.* **43** 216

[57] Mehmood F, Hoffmann M, Lomenzo P D, Richter C, Materano M, Mikolajick T and Schroeder U 2019 *Adv. Mater. Interfaces* **6** 1901180

[58] Gong N and Ma T P 2016 *IEEE Electron. Device Lett.* **37** 1123